

2008

Explanation of magnetic behavior in Ru-based superconducting ferromagnets

Rashmi Nigam

University of Wollongong, rnigam@uow.edu.au

Alexey V. Pan

University of Wollongong, pan@uow.edu.au

S X. Dou

University of Wollongong, shi@uow.edu.au

Follow this and additional works at: <https://ro.uow.edu.au/engpapers>



Part of the [Engineering Commons](#)

<https://ro.uow.edu.au/engpapers/1793>

Recommended Citation

Nigam, Rashmi; Pan, Alexey V.; and Dou, S X.: Explanation of magnetic behavior in Ru-based superconducting ferromagnets 2008, 134509-1-134509-9.

<https://ro.uow.edu.au/engpapers/1793>

Explanation of magnetic behavior in Ru-based superconducting ferromagnets

R. Nigam, A. V. Pan, and S. X. Dou

Institute for Superconducting and Electronic Materials, University of Wollongong, Northfields Avenue, Wollongong, New South Wales 2522, Australia

(Received 28 October 2007; revised manuscript received 13 February 2008; published 11 April 2008)

We have investigated $\text{RuSr}_2\text{Eu}_{1.5}\text{Ce}_{0.5}\text{Cu}_2\text{O}_{10}$ (Ru-1222) and $\text{RuSr}_2\text{EuCu}_2\text{O}_8$ (Ru-1212) samples by using x-ray diffraction, scanning electron microscopy, dc magnetization, ac susceptibility, and resistivity measurements. Based on the results obtained, we propose an explanation of the magnetic behavior of the Ru-based systems. Our model is capable of describing controversial observations of multiple magnetic transitions on temperature dependent dc magnetization measurements as well as the reentrance of irreversibility in hysteresis loops at high temperatures, which enables the bell-shaped behavior of the coercive field within $90\text{ K} \leq T \leq 200\text{ K}$. The experimental results suggest that Ru-based samples always contain a small amount of at least one additional magnetic phase with its own magnetic behavior, which is similar yet distinct from the main Ru phase. The presence of these phases and the superposition of their magnetic contributions can produce different transport properties and lead to features that are inherent to various magnetic states, such as ferromagnetic, antiferromagnetic, and spin glass, and still exhibit a coexistence of magnetism and superconductivity at low temperatures. This variety of possible states has led to different controversial models proposed in the literature, reflecting one or another feature observed. The model proposed in this work does not contradict but rather unifies the existing scenarios for the Ru-based systems in a common picture.

DOI: [10.1103/PhysRevB.77.134509](https://doi.org/10.1103/PhysRevB.77.134509)

PACS number(s): 74.25.Qt, 74.25.Op, 74.25.Ha, 74.72.Jt

I. INTRODUCTION

Superconductivity (SC) and magnetism were considered to be mutually exclusive phenomena in a material before a region of coexistence was observed at very low temperatures in superconducting tertiary rare earth compounds [RRh_4B_4 , RMO_6S_8 , RMO_6Se_8 ,¹ and $\text{RNi}_2\text{B}_2\text{C}$ (Ref. 2) systems, with R being the rare earth elements], $\text{CeRh}_{1-x}\text{Co}_x\text{In}_5$, URhGe , and ZrZn_2 . The most recent discovery was the observation of a coexistence of SC and magnetism in rutheno-cuprate materials, which belong to the class of high temperature superconductors. The two types of rutheno-cuprate materials are $\text{RuSr}_2\text{R}_{2-x}\text{Ce}_x\text{Cu}_2\text{O}_{10}$ (Ru-1222) (Refs. 3 and 4) and $\text{RuSr}_2\text{RCu}_2\text{O}_8$ (Ru-1212),^{5,6} where R is Eu, Gd, or Sm. In these compounds, superconductivity appears when a system is in a ferromagnetic (FM) state; hence, they are called superconducting ferromagnets. In both Ru-1222 and Ru-1212, magnetism originates from the RuO_2 sheet or, more precisely, from the RuO_6 octahedra, whereas superconductivity is supposed to reside in CuO_2 planes. Both the superconducting and magnetic layers are practically decoupled, which accounts for the mutually exclusive yet coexisting nature of these two phenomena. At the same time, it casts doubts on the genuine coexistence of these phenomena at the microscopic level.

Compared to Ru-1222, Ru-1212 is more intensively studied. As reported in literature for Ru-1212, the superconducting transition (T_c) takes place between 18 and 46 K,^{5,6} which is way below the magnetic transition temperature. Neutron diffraction studies suggested that antiferromagnetic (AFM) transition occurs at 133 K with a small FM component arising due to canting of Ru ions,⁷ whereas magnetization measurements and nuclear magnetic resonance experiments⁸ proposed a strong FM component. Due to the fact that large discrepancies between different studies have been found, no

final conclusion has been drawn yet on the magnetic behavior observed. A similar case is found for the Ru-1222 system, which has a much more complicated magnetic behavior in comparison to Ru-1212. In contrast to a single magnetic transition at 133 K in the Ru-1212 system, Ru-1222 undergoes multiple magnetic transitions with an unclear origin, making it a more difficult system to understand.^{3,4,9,10} However, a commonly recognized feature in Ru-1222 (just like in Ru-1212) is the coexistence of superconductivity, which sets in at $T_c \sim 20\text{--}50\text{ K}$,^{3,4} and ferromagnetism below the Curie temperature (T_C). Note that the upper case subscript notation is used for the Curie temperature, whereas the lower case subscript notation is for the superconducting transition. A spin glass behavior has also been hypothesized in Ru-1222 as a result of a combined effect of antiferromagnetism and ferromagnetism.^{11,12} Generally, various studies on Ru-1222 made by different groups show inconsistent results; hence, different scenarios have been proposed to explain the magnetic transitions observed.

The existing explanations of the inconsistent magnetic behavior found in the Ru-based systems have not been clearly distinguished for the Ru-1212 or the Ru-1222 system, which might be another reason for the different interpretations. One can find the following interpretations of the magnetic behavior in Ru-based systems:

(i) One scenario proposed in Ref. 5 is based on zero-field muon-spin rotation (μSR) and magnetization experiments in the Ru-1212 ($\text{RuSr}_2\text{GdCu}_2\text{O}$) system. This scenario assumes that the Ru-1212 material exhibits a microscopically homogeneous FM order below the Curie temperature. At a much lower temperature, the system also becomes superconducting below the superconducting transition ($T_c \sim 16\text{ K}$), presuming that superconductivity relies on the two-dimensional charge dynamics of the CuO_2 planes, whereas the ferromagnetic order of Ru moments is confined to the RuO_2 planes. Above $T_c \sim 133\text{ K}$, the system is paramagnetic. Antiferro-

magnetic ordering of Gd moments is also assumed to occur below the Néel temperature ($T_N \sim 2.6$ K).

(ii) Another scenario is proposed in Refs. 13 and 14 for the results obtained for the Ru-1222 system $[\text{RuSr}_2(\text{Gd}, \text{Ce})_2\text{Cu}_2\text{O}_{10-\delta}]$. This scenario suggests a possible phase separation, which is assumed to reconcile the controversial results explained by the canting Ru spins¹⁵ in the homogeneous phase [scenario (i)].¹³ This phase separation proposes FM species coexisting with a possible AFM matrix within crystal grains. The paramagnetic matrix becomes antiferromagnetic at T_{M1} , which is considered to be the main transition occurring at ~ 80 K. Meanwhile, two ferromagnetic transitions occur at $T_{M2} \sim 120$ K and $T_{M3} \sim 140$ K. Note that the three transitions reported may actually assume a threefold phase separation (including AFM matrix).

(iii) A third scenario⁹ for $\text{RuSr}_2\text{Eu}_{1.5}\text{Ce}_{0.5}\text{Cu}_2\text{O}_{10}$ is claimed to be a combination of the two scenarios outlined above. It also deals with phase separation, so that a minor phase (comprising about 15%) starts to order with antiferromagneticlike features at $T_M \sim 125$ K for Ru-1222 and the majority fraction becomes weakly ferromagnetically ordered at $T_{M2} \sim 80$ K. Such a phase separation is assumed to occur due to either an inhomogeneity in the oxygen content, so that a minor fraction of Ru^{+5} ions is reduced to Ru^{+4} islands with the transition at T_M while a major fraction of the Ru^{+5} ions orders at T_{M2} , or to the presence of some Sr-Cu-Ru-O impurity phase. Note that the notations, such as T_M , T_{M1} , etc., are taken directly from the corresponding references and, hence, may not denote the same transitions, which is also quite confusing.

In addition, the nature of the multiple magnetic transitions has been attributed to the intrinsic features of the Ru-1222 system.^{9,16,17} However, the phase separation interpretations proposed along with the fact that these multiple transitions can be absent or strongly suppressed in the dc magnetization measurements^{1,18,19} cast doubts on the validity of the intrinsic nature of the transitions.

In this work, we propose the explanation of the magnetic behavior in Ru-based systems based on our magnetic and resistivity measurements as well as structural experiments, which may resemble all of the three aforementioned scenarios depending on the features of a particular Ru system (1212 vs 1222) or/and sample preparation routine. We also provide evidence that the multiple magnetic transitions observed are most likely an extrinsic feature, which arises due to the sophisticated element structure of the material as well as the imperfect preparation conditions, which can be difficult to overcome completely.

II. EXPERIMENTAL DETAILS

The samples of $\text{RuSr}_2\text{Eu}_{1.5}\text{Ce}_{0.5}\text{Cu}_2\text{O}_{10}$ (Ru-1222) were synthesized through a solid-state reaction route from the stoichiometric amounts of 99.99% pure RuO_2 , SrCO_3 , Eu_2O_3 , CeO_2 , and CuO . A series of samples with the same stoichiometry was prepared with the same intermediate heat treatments at 1000, 1020, and 1040 °C for 12 h, but different final sintering temperatures. The samples were pressed into circular pellets. The pellets were then annealed at 600 °C in

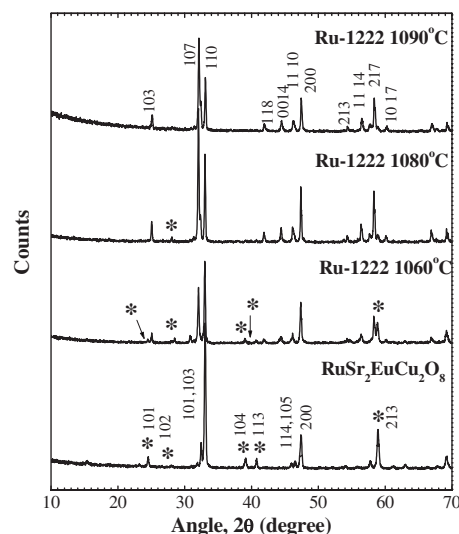


FIG. 1. XRD patterns of the Ru-1222 samples prepared at 1060, 1080, and 1090 °C, and the Ru-1212 sample.

flowing oxygen for 48 h and, subsequently, slowly cooled over a span of another 24 h down to room temperature. $\text{RuSr}_2\text{EuCu}_2\text{O}_8$ (Ru-1212) samples were also prepared by using the same procedure mentioned above, but with the final sintering temperature of 1080 °C. X-ray diffraction (XRD) patterns were measured by using a Philips PW1730 with $\text{Cu } K\alpha$ radiation. The dc magnetic measurements were performed by using a Magnetic Property Measurement System (MPMS-XL, Quantum Design) in the temperature range of 1.9–300 K. ac susceptibility measurement with varying frequency and fixed ac magnetic field as well as four-probe resistivity measurement were carried out inside the cryostat of a Physical Property Measurement System (Quantum Design). The microstructure was observed by using a field-emission scanning electron microscopy (SEM) unit (JEOL JSM-6700F).

III. RESULTS

Three Ru-1222 samples having different final sintering temperatures, namely, 1060, 1080, and 1090 °C, are chosen for the discussion. Figure 1 shows the XRD pattern for these Ru-1222 samples. The XRD pattern of the 1060 sample shows that the Ru-1222 phase is not pure, since a number of impurity peaks have been observed at $2\theta = 24.5^\circ$, 39° , 40.7° , 58.8° , and 63° , which correspond to (101), (102), (104), (113), and (213) reflections of the Ru-1212 phase.¹⁸ After increasing the final sintering temperature from 1060 to 1080 °C, the phase composition has been significantly improved with only one detectable impurity peak at $2\theta = 28^\circ$. A further 10 °C increase to 1090 °C in the final sintering temperature has resulted in the phase pure Ru-1222 material, according to the XRD results. Both Ru phases possess a tetragonal structure, with Ru-1222 belonging to the $I4/mmm$ space group and Ru-1212 to the $P4/mmm$ space group. The list of the lattice parameters and the amounts of the two phases present²⁰ in the samples are given in Table I.

TABLE I. The crystal lattice parameters of Ru-1222 sintered at different temperatures and Ru-1212 sample, the percentage of Ru-1212 secondary phase present in Ru-1222 samples and their T_c and T_{cusp} obtained from dc magnetization measurements, and T_c calculated from the temperature dependence of saturation magnetization are provided. All of the values of temperature are in Kelvin.

Sample	$a=b$	c	% Ru-1212	T_c	T_{cusp}	T_{irr}
1060 °C	3.93033	29.3111	14.6	37	74	200
1080 °C	3.84398	28.5957	4.8	27	74	160
1090 °C	3.84580	28.5919		25	72	160
1212	3.84601	11.5486				200

Zero-field cooled (ZFC) and field cooled (FC) dc magnetization measurements were carried out for these three Ru-1222 samples with different purity levels (Fig. 2). In general, the behavior of the pure (1090) and nearly pure (1080) samples are quite similar [Figs. 2(b) and 2(c)] and can be divided into the three following regions: first, a weakly temperature dependent region ($T > 95$ K) presumably above the

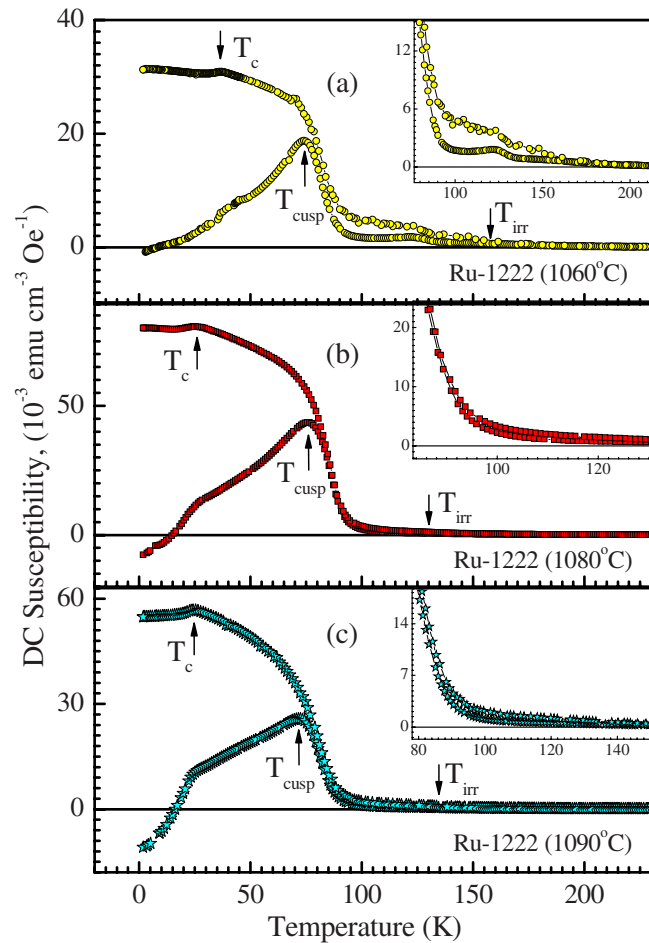


FIG. 2. (Color online) ZFC and FC dc magnetization curves of (a) 1060 °C, (b) 1080 °C, and (c) 1090 °C sintered samples of $\text{RuSr}_2\text{Eu}_{1.5}\text{Ce}_{0.5}\text{Cu}_2\text{O}_{10}$ measured at 10 Oe. The inset shows the enlarged view of the curves above T_{cusp} marked by one of the arrows in (a).

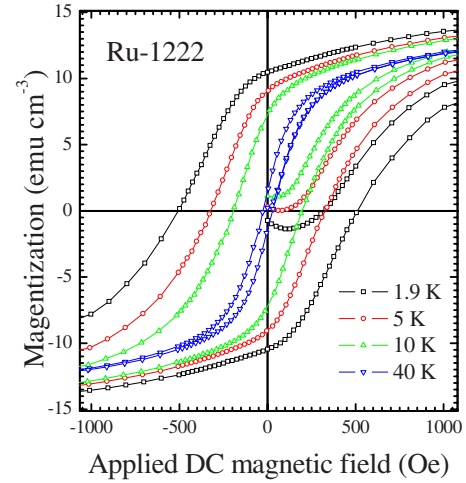


FIG. 3. (Color online) Typical magnetization loops as a function of applied magnetic field measured at different temperatures for the Ru-1222 samples.

Curie temperature. Second, the susceptibility steeply rises, exhibiting a rather conventional ferromagnetic behavior with irreversible ZFC and FC curves, so that the ZFC curve shows a peak (denoted as T_{cusp}), whereas the FC curve exhibits a gradual increase with decreasing temperature. Third, at about 27 K, both ZFC and FC curves exhibit a kink, which represents the superconducting transition, so that below about 15 K a Meissner-type diamagnetic signal is obvious for the ZFC curve. The parameters measured for the samples are given in Table I. Clearly, the impure sample (1060) shows at least two distinctly different features [Fig. 2(a)], namely, the pronounced irreversibility sets in at a much higher temperature ($T_{\text{irr}} \sim 200$ K) than in the “pure” samples ($T_{\text{irr}} \sim 160$ K) and there is a clear peaklike anomaly observed at about 124 K for both ZFC and FC curves. However, a more careful study (see the insets in Fig. 2) shows that the pure samples also have a small irreversibility above the Curie temperature. This small irreversibility, in contrast to the impure sample, vanishes before the reopening, which can clearly be seen for ZFC and FC curves in the vicinity of T_{cusp} . In this work, we have determined the Curie temperatures for the samples by plotting the saturation magnetization (M_{sat}) as a function of temperature [Fig. 4(a)]. The temperature at which M_{sat} becomes zero is identified as the Curie temperature (T_c). More specific details on defining T_c are provided later on in the text.

Hysteresis loops $M(H)$ for the Ru-1222 samples have been measured in the temperature range between 5 and 300 K and over the applied magnetic field range of $|H| \leq 50$ 000 Oe (Fig. 3). Generally, the loops show a ferromagneticlike behavior, which coexists with the Meissner (diamagnetic) signal at $T < T_c$ and low applied fields. This provides another fact, in addition to the $\chi(T)$ behavior, confirming the coexistence of superconductivity and ferromagnetism. Furthermore, to understand the nature of the irreversibility, we have plotted the coercive field H_c as a function of temperature in Fig. 4(b). In agreement with $\chi(T)$, the $H_c(T)$ curves exhibit a coercive field at low temperatures, which vanishes at $T \approx 60$ K for all of the samples. At $T \approx 80$ K, the coercivity reemerges with a bell-like shape, which is pro-

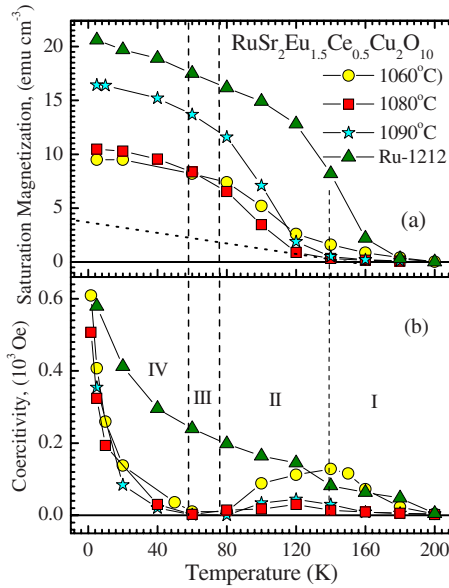


FIG. 4. (Color online) Temperature dependence of (a) the saturation magnetization (M_{sat}) and (b) the coercive field (H_C) for the Ru-1212 and Ru-1222 samples. The dashed lines mark approximate boundaries between the different zones. The dotted line is the imaginary $M_{\text{sat}}(T)$ extension of the secondary FM phase (Ru-1212) present.

nounced for the impure sample and is strongly suppressed (but visible) for the pure samples. Eventually, the coercivity completely vanishes at ≈ 160 K for the pure samples and at ≈ 200 K for the impure sample. A bell-like shape has also been reported to appear or disappear depending on the stoichiometric composition of the Ru-1222 samples,^{9,10} whose preparation may lead to a varying impurity content.

The hysteresis loops have also enabled the analysis of the temperature dependence of the saturation magnetization [Fig. 4(a)], which is conventionally determined at the intersection of the extension line of the saturated magnetization with the magnetization axis. A typical ferromagnetic behavior^{9,19} of the $M_{\text{sat}}(T)$ curves exhibits $T_C \approx 120$ K. However, it can be seen that M_{sat} does not completely vanish at 120 K. At this temperature, $M_{\text{sat}}(T)$ abruptly changes the slope, which vanishes at about 200 K for the impure sample and at about 160 K for the pure samples. This kind of behavior may indicate two superposed magnetic phases: a major phase with vanishing saturation at 120 K and a minor phase with vanishing saturation at $T \geq 160$ K. The imaginary $M_{\text{sat}}(T)$ of the minor phase is denoted by a dotted line below 120 K in Fig. 4(a) for a better visualization of this superposition.

Thus, the irreversibility above the Curie temperature, the bell shape of $H_C(T)$, and the observed behavior of the $M_{\text{sat}}(T)$ curves are likely characteristic features associated with the structural composition of the samples investigated. Moreover, our results are in agreement with the ⁵⁷Fe and ¹¹⁹Sn Mössbauer spectroscopy,¹⁰ showing the presence of two distinct magnetic phases, as well as with muon-spin rotation studies.¹⁷ Muon-spin rotation studies were carried out on RuSr₂Eu_{1.4}Ce_{0.6}Cu₂O₁₀ samples, whose magnetization behavior was reminiscent of our impure sample. These μ SR results have indicated that $\sim 15\%$ of the sample volume com-

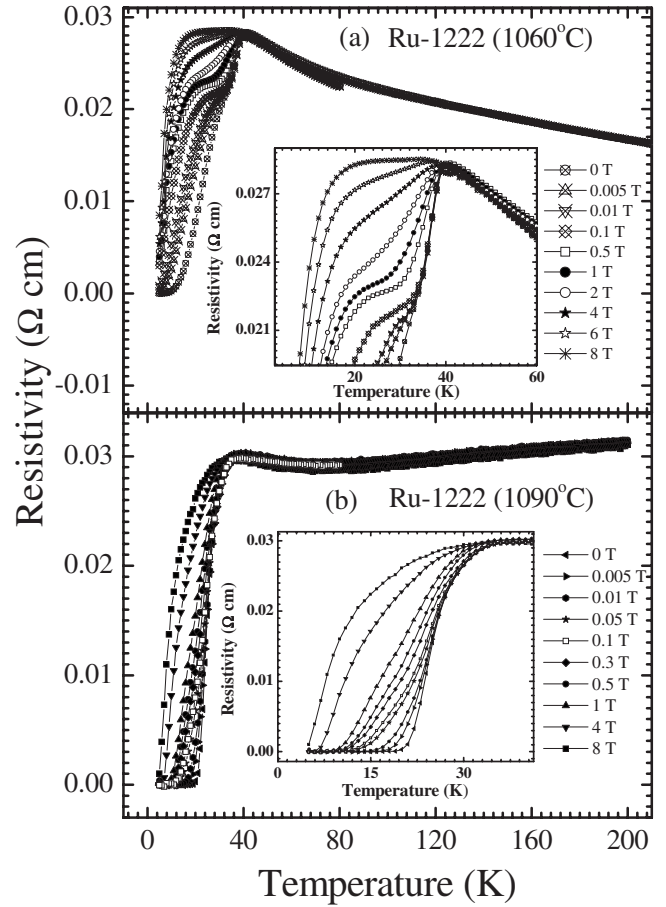


FIG. 5. Resistivity as a function of temperature for the (a) 1060 °C (impure) and (b) 1090 °C (pure) Ru-1222 samples at applied fields $H \leq 8 \times 10^4$ Oe. The inset shows the enlarged view of a superconducting transition.

prises some minority phase, which orders magnetically below ~ 200 K. Note that this volume of impurities is consistent with the percentage of the Ru-1212 secondary phase in the impure sample estimated²⁰ from the XRD results in Fig. 1 and given in Table I.

Another clear experimental evidence of the presence and influence of the Ru-1212 phase on the behavior of the Ru-1222 system is brought forward by investigating its resistivity (Fig. 5) over the temperature range of 5–300 K and the applied field range of $0-8 \times 10^4$ Oe. Particularly informative is the superconducting transition, which exhibits a clear double-step transition for the impure sample, which eventually evolves into the single-step transition for the pure sample (1090). Moreover, the impure sample shows a semiconductorlike behavior above T_c with an exponential curvature, whereas the pure sample has a metalliclike behavior with a linear dependence. This behavior is governed by changing the amount of the secondary Ru-1212 phase (found by XRD) between the Ru-1222 grains and, hence, modifying the granularity (Fig. 6).¹⁸ The Ru-1222 grains can become superconducting at a higher superconducting transition temperature than that of the minority Ru-1212 phase, which can have the transition at a lower temperature, leading to the double-step transition. The pure sample shows a single-step

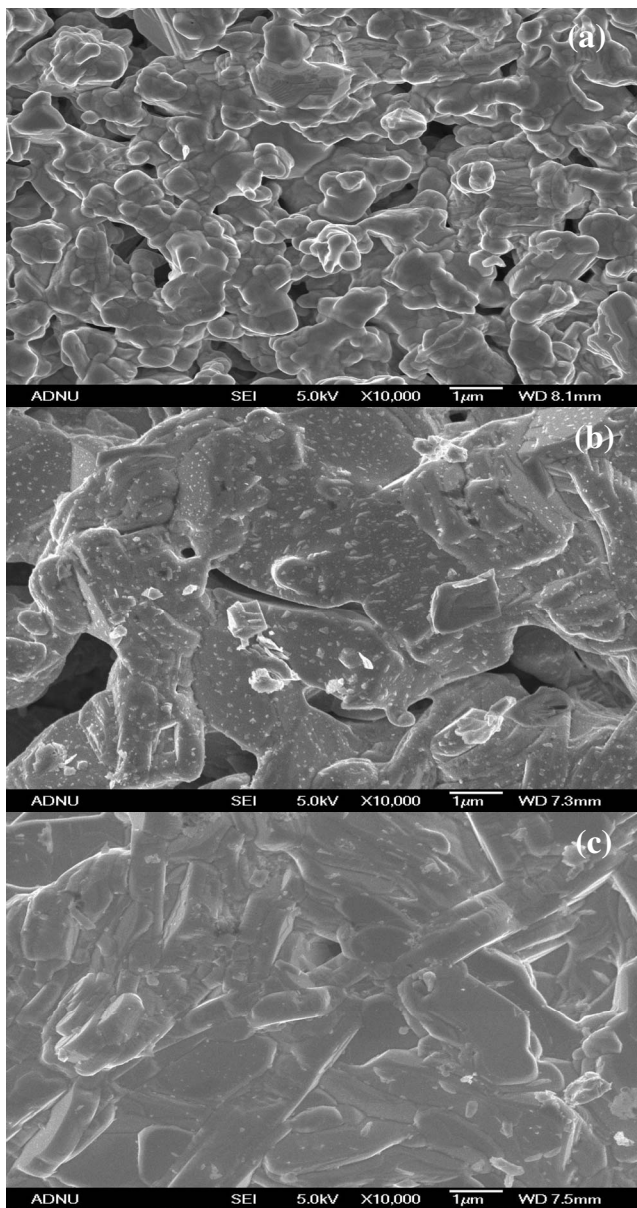


FIG. 6. SEM images of the microstructure for the (a) 1060 °C, (b) 1080 °C, and (c) 1090 °C samples of Ru-1222.

transition since the secondary phase, to a large extent, is absent. The SEM observation of sample microstructures illustrates that the impure Ru-1222 has well defined small grains (typically $\sim 2 \mu\text{m}$) with pronounced grain boundaries. This leads to the semiconductorlike behavior of the resistivity. The pure Ru-1222 sample exhibits a more uniform structure with large grains and hardly visible grain boundaries, which lead to the metalliclike curve.

Thus, we can summarize our experimental data presented above by noting that a magnetic impurity (or secondary) phase, likely Ru-1212, does affect the structural, magnetic, and transport properties of the Ru system and the explanations of the measurement results. Moreover, the simplicity in the manipulation of the results by changing the temperature of the final heat treatment suggests a possible common explanation (discussed in Sec. IV) of the range of seemingly

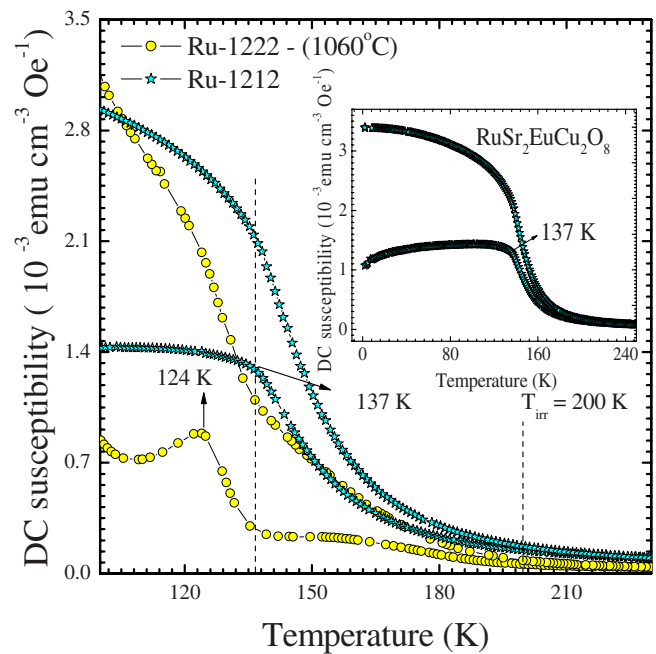


FIG. 7. (Color online) Enlarged comparison of the magnetization curves for Ru-1212 and the impure Ru-1222 samples. The inset shows the ZFC-FC magnetization curve as a function of temperature for Ru-1212.

inconsistent and controversial results available in the literature, which reports typical features of either the impure sample^{9,16,17} or the pure samples.^{1,19}

We can now separate the contributions of each (1212 and 1222) system and correspondingly establish the extent to which both contributions affect the overall magnetic behavior. We know the signal of our 1212/1222 composite system in the impure sample, we know the 1222 signal of our pure sample (both shown in Fig. 2), and, in addition, we have measured ZFC and FC dc magnetization curves of the 1212 sample (the inset of Fig. 7). The dc susceptibility behavior of Ru-1212 shows a typical ferromagnetic behavior.²¹ The dependence of the coercive field on temperature [Fig. 4(b)] shows a monotonous increase in coercivity, which indicates the hardening of the ferromagnetic-type behavior with decreasing temperature. In general, the dc susceptibility, $M_{\text{sat}}(T)$, and $H_C(T)$ for Ru-1212 behave in a similar way as those for the pure Ru-1222 [see Figs. 2, 4(a), and 4(b)]. Comparing these dependences between the 1212 and pure 1222 systems, we can see that H_C and M_{sat} for both Ru-1212 and impure Ru-1222 start to appear at 200 K, whereas for pure Ru-1222, these appear at 160 K. Hence, we can conclude that the magnetic behavior for both phases has a similar origin. Note that as soon as we “add” a 1212 impurity phase to a 1222 impurity phase for the 1060 °C sample, its irreversibility increases to 200 K as in the case of the 1212 sample. This shows that the variation in the magnetic transition temperatures of different Ru-1222 samples depends on the amount of the Ru-1212 impurity phase present which, in turn, depends on the preparation conditions.

To give a full picture, we should also note that the XRD pattern of the Ru-1212 sample (Fig. 1) shows an impurity peak at $2\theta=32^\circ$ corresponding to another ferromagnetic

phase (SrRuO_3) with a Curie temperature of ~ 165 K.^{22,23} Although it was argued that the SrRuO_3 impurity has no prominent effect on the magnetic behavior of the 1212 phase,²² we have not verified its role in the magnetic behavior for either of the Ru systems. However, we emphasize that the XRD pattern shows that some amount of SrRuO_3 is present in both impure and pure Ru-1222 samples. In addition, the presence of a minute amount of other Sr-Ru-O impurities in the 1222 samples may not be ruled out despite the fact that they remain unresolved by XRD. Thus, the temperature for irreversibility may vary for both phases depending on the processing temperature. This is observed in our experiments. Moreover, the presence of SrRuO_3 in the Ru-1222 sample containing the Ru-1212 phase and in the Ru-1222 sample that is free of the Ru-1212 phase suggests that the anomalous magnetic features (i.e., the bell shape of H_C and the small peak near 125 K) observed in the magnetic behavior of the Ru-1222 samples containing the Ru-1212 phase comes from the influence of the Ru-1212 impurity phase, rather than from the SrRuO_3 phase.

Thus, we now have all the magnetic signal components that presumably contribute to the magnetic behavior for the pure and impure samples. In the next section, we suggest a model that explains the behavior of the Ru-based systems investigated, as well as establishes the connection between the models suggested in the literature and the present observations.

IV. MODEL

The experimental results described in the previous section allow us to propose a simple model that will explain our results with respect to the multiple magnetic transitions particularly for 1222 system [Fig. 2(a)] and will not contradict but, moreover, unify the models suggested in the literature.^{5,9,13,14,16,17,19}

Although we believe that the behavior of the Ru-1212 and Ru-1212 systems is generally quite similar, however, our model makes a clear cut between them in order to explicitly explain the situation.

A. Ru-1212

This system possesses all of the features that allow us to define it as being ferromagnetic below the Curie temperature $T_C \approx 200$ K, as can be seen in the inset of Fig. 7. Above T_C , the system behaves as a paramagnet with a characteristic reversible linear $M(H)$. Below T_C , it shows a ferromagnetic history dependence with ZFC/FC irreversibility, which is characteristic of ferromagnetic transition.²¹ In fact, this description reproduces scenario (i)⁹ outlined in Sec. I. The relatively high Curie temperature might be associated with the notable amount of the SrRuO_3 impurity phase due to the particularities of the sample preparation. Moreover, the significant variation in oxygen content of different samples may alter the transition temperature and the amount of impurities. In the absence of this impurity, the Curie temperature could have been (140 ± 10) K as in Refs. 9 and 22.

For this phase, we experienced perhaps the only controversy that remained unexplained. In Ref. 22, a behavior simi-

lar to the one we have observed and explained as being ferromagnetic was described as antiferromagnetic. The reason for this interpretation remains unclear, but could be associated with the sample preparation.

B. Ru-1222

Having established the features of the Ru-1212 behavior, we can now explain seemingly even more controversial results for the 1222 phase. Relying on the combination of our XRD, SEM, magnetization, and resistivity measurements, we can conclude that Ru-1222 generally behaves in the same way as its Ru-1212 counterpart. It is paramagnetic above $T_C \approx 120$ K [Fig. 4(a)] and ferromagnetic below T_C , exhibiting the characteristic magnetic history dependent ZFC and FC curves [Figs. 2(b) and 2(c)] similar to those of the 1212 material (Fig. 7). In fact, the behavior of $M_{\text{sat}}(T)$ [Fig. 4(a)], $H_C(T)$ (Fig. 4), and $M(H)$ (Fig. 3) for the pure samples (1080 and 1090) is similar to that for 1212.

The origin of the multiple magnetic transitions in 1222 [Fig. 4(a)] is directly associated with the presence of the 1212 impurity (the second magnetic species, following terminology of Refs. 13 and 14). As the level of the impurity is substantially reduced in the pure samples (1080 and 1090) as compared to that of the 1060 impure sample (Table I), the controversial additional transition visible as an additional peak at about 124 K in Fig. 2(a) vanishes. This conclusion is very clearly supported by a vanishing double step in the resistivity at the superconducting transition for the pure samples (Fig. 5).

The magnetization measurements on the 1222 system show that $T_C \approx 120$ K [Fig. 4(a)] does not depend on the purity of the samples, and T_C shows up on the $\chi(T)$ curves (Fig. 2) as a sharp rise of the dc susceptibility just below 100 K. For the 1212 system, $T_C \approx 160$ K [Fig. 4(a)] and it shows up as a rise of the dc susceptibility below ~ 160 K. A similar T_C is also observed for the impure 1222 sample that has 1212 impurities [Fig. 4(a)]. This secondary T_C is accompanied by a small peak at ~ 124 K [Fig. 2(a)]. Overall, the superposition of two ferromagnetic signals in the 1222 samples that contain any amount of 1212 impurity becomes obvious in the $\chi(T)$ and $M_{\text{sat}}(T)$ dependences. Indeed, the presence of the remnant irreversibility above 120 K for the pure samples (the insets to Fig. 2) and the XRD results for the nearly pure sample (1080 °C) indicate that there could be minor remnant traces of the 1212 phase even for the pure sample. Thus, we can call the transition at 160 K as intrinsic^{16,17} to the 1222 system only in the sense that all the attempts to prepare a 100% pure 1222 phase were *unsuccessful* so far. Thus, the multiple magnetic transitions within $90 \text{ K} \lesssim T \lesssim 200 \text{ K}$ are likely to originate from the superposition of two ferromagnetic signals: a dominating signal from 1222 and a signal from the minority 1212 phase.

In the preceding section, we have found the magnetic signals of 1222 and 1212 systems measured at $H=10$ Oe for the pure 1222 sample (1090) and the 1212 sample, which are respectively shown in Fig. 2(c) and in the inset of Fig. 7. These signals are assumed to contribute to the magnetization of the impure 1222 sample. Now, in Fig. 8, we show the

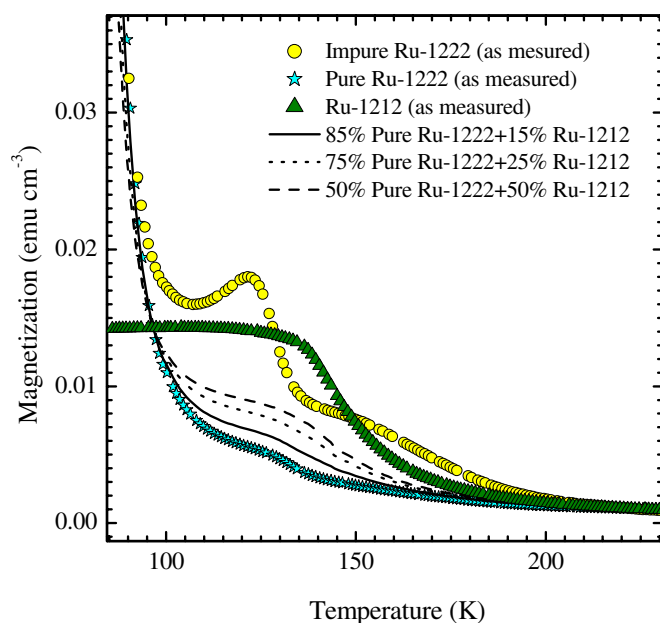


FIG. 8. (Color online) The solid, dashed, and dotted lines are the result of a direct summation of ZFC magnetization curves measured separately at $H=10$ Oe for the pure Ru-1222 and Ru-1212 samples with different weighting factors corresponding to the different 1212 impurity levels in the impure 1222 system. The ZFC curve measured at the same conditions for the impure 1222 sample with 15% of 1212 impurities exhibiting a peak near 125 K is shown as well (solid line).

result of the direct summation of these two ZFC signals with different weightings, which would correspond to a different amount of 1212 impurities in the 1222 sample. According to our XRD results, the amount of the 1212 impurity is about 15% (solid line in Fig. 8). A similar approach was used to separate two magnetic signals in a bulky superconductor/ferromagnet composite.^{24,25} As can be seen, the resultant curves exhibit a distinct feature that may somewhat resemble the behavior of the impure 1222 sample (1060) with two magnetic transitions shown in Fig. 8 for comparison: the enhancement at around ~ 140 K (corresponding to 1212) and below 100 K (corresponding to 1222). Thus, the amount of the 1212 impurity observed in the impure 1222 sample (1060) is clearly sufficient to appear as a double transition in the magnetization curve. In addition to the magnetic superposition, Ru^{4+} - Ru^{5+} spin interactions⁶ in Ru-1222 (where Ru is known to exist in the pentavalent state) and in Ru-1212 [where Ru exists in mixed (4+) and (5+) valence states²⁶] have been proposed to create a small peak and a pronounced irreversibility [scenario (iii)]. Note that there is no contradiction between the magnetic superposition model and this scenario assuming oxygen content variation.⁹ Indeed, 1212 and 1222 phases do have different oxygen content. As the 1212 phase is likely to reside inhomogeneously around 1222 grains¹⁸ (and possibly within the grains), it can be measured as an inhomogeneity in oxygen content, which would then involve scenario (iii). It is noteworthy that the peak marking the transition for 1212 in the impure 1222 sample might be stronger as a result of an enhanced spin orientation in the canted 1222 areas adjacent to the 1212 impurity. This en-

hancement cannot happen if we directly add two signals measured separately. Moreover, as discussed below, the mixture of two magnetic phases may also lead to the formation of a spin glass state, impacting the magnetization behavior as well.

As a matter of fact, the $M_{\text{sat}}(T)$ and H_C curves of the impure sample 1060 °C shows another feature that is consistent with the corresponding curves of the 1212 sample, terminating not at 160 K but at 200 K (Fig. 4). This fact may be attributed either to the particularities of the preparation procedure and the corresponding structural differences associated with it,⁶ or to the possible presence of the somewhat enhanced amount of the SrRuO_3 (or another) impurity phase with $T_C \approx 200$ K in both samples.¹⁷ In fact, a possible presence of both 1212 and SrRuO_3 impurity phases in the main 1222 phase may explain the three transitions observed in Refs. 13 and 14.

To complete the explanation of the magnetic behavior as the superposition of the magnetic responses of the 1212 and 1222 phases, we should be able to explain the disappearance of the irreversibility [i.e., $H_C=0$ in Fig. 4(b)] over the temperature range of $60 \leq T \leq 80$ K as well as the bell shape of the $H_C(T)$ over the range of $80 \leq T \leq 200$ K.

The most straightforward explanation has region IV below ~ 60 K. In this region, H_C rapidly rises for all of the 1222 samples from nearly 0 to about 0.06 T at 1.9 K. This rise indicates that Ru-1222 undergoes a significant FM “hardening” below 60 K due to decreasing thermal activation energy, which promotes the FM alignment of Ru spins.

A similar increase of H_C shows the impure Ru-1222 below 200 K in region I, but, in this case, the rising value of H_C is governed by the FM ordering of the 1212 impurity clusters. This may be supported by muon-spin rotation experiments,¹⁷ according to which an unidentified minor volume fraction undergoes magnetic ordering at 200 K. In contrast, the pure samples (1080 and 1090) exhibit considerably suppressed H_C values within the range of $80 \leq T \leq 200$ K (regions I and II). As mentioned above, the remanent irreversibility (and corresponding $H_C \neq 0$) is likely due to some remanent traces of the Ru impurity phases.

As a result of the superposition of two ferromagnetic signals in the impure Ru-1222, one might expect to see a behavior similar to that observed for $M_{\text{sat}}(T)$ in Fig. 4(a) with a change in the slope of rising H_C at the temperature of about 120 K when the FM ordering starts for the 1222 phase. Instead, we observe the opposite: upon decreasing temperature, H_C starts to decrease at 120 K and completely disappears at 80 K before starting to rise again at ~ 60 K. The explanation to this behavior might be the following. In the vicinity of the peak of the $H_C(T)$ “bell,” the 1222 phase has its FM transition with the Curie temperature of 120 K. As a result, the system would consist in the superposition of two ferromagnetically ordered phases so that the net spin interaction exhibits a decrease in coercivity, which can be observed in AFM compounds. Thus, we may confer that the impure Ru-1222 system may develop an AFM-like character in region II. In other words, the two coexisting FM phases produce a net AFM-like, most likely nonmicroscopical, ordering. Moreover, the bordering regions between these two phases may experience a local reorientation of spins,^{27,28} also lead-

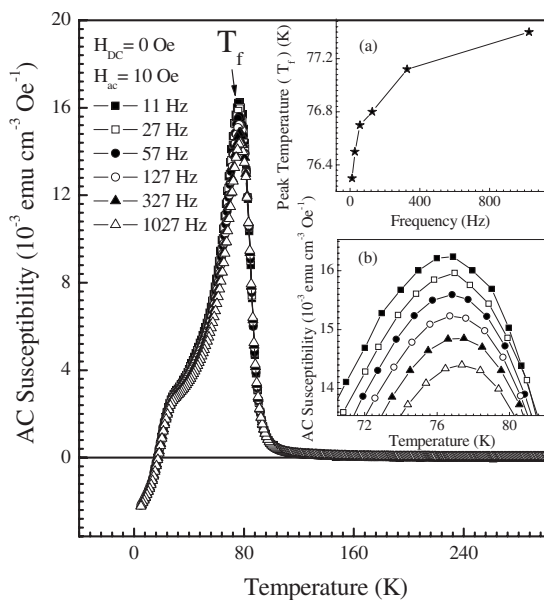


FIG. 9. Temperature dependence of the ac susceptibility measured at different frequencies of the applied ac field for the Ru-1222 (1060) sample. The inset shows the frequency dependence of (a) peak temperature (T_f) and (b) peak height.

ing to a glassy spin arrangement which can start at ≈ 120 K (the peak of the bell). As the FM behavior of the dominating 1222 phase hardens with decreasing temperature, the overall spin arrangement in the system can arrive at a spin glass state at about 80 K with $H_C \approx 0$, which manages to survive down to lower temperatures. At the point $H_C \approx 0$, the hardened ferromagnetic behavior of the 1222 phase takes over and the characteristic increase in H_C with decreasing temperature is observed. Note that, at about 120 K, most of the 1212 phase (comprising about 15% of the sample) exhibits ferromagnetism, while the FM ordering in the dominant 1222 phase just commences, enabling a notable impact from both phases between 120 and 80 K. The above explanation can also be provided in terms of different oxygen contents in various clusters as proposed in Ref. 9 since 1212 and 1222 phases do have different oxygen contents.

To reinforce our arguments about the existence of the spin glass state, we have measured the ac susceptibility (χ_{ac}) as a function of temperature at different frequencies (f) and at an applied ac field $H_{ac} = 10$ Oe (Fig. 9). The ac susceptibility curve shows a pronounced peak at temperature $T_f \approx 76$ K, which is called the freezing temperature of the spins. In this state, this peak is frequency dependent, which is characteristic of a spin glass behavior.¹¹ In the inset of Fig. 9, it can be seen that upon increasing frequency, the peak position shifts slightly toward higher temperatures, whereas the height of the peak decreases. The shift of T_f and frequency dependence of the peak height lies below 80 K, which corresponds to region III, where the spin glass behavior originates, extending to lower temperatures in region IV. In addition, we note that $\chi_{ac}(T)$ curves exhibit an insignificant frequency dependence just below 120 K, indicating a possibility of the onset of some local glassy regions.

V. CONCLUSION

We have developed a model of the magnetic behavior in Ru-1212 and Ru-1222 systems, which has enabled us to explain this behavior as well as to unify the controversial results and explanations proposed in the literature. The main finding is that the magnetic behavior in Ru-1222 is governed by the superposition of two ferromagnetic signals from a dominating 1222 phase and a minor 1212 phase. This superposition underpins a range of sophisticated magnetic interplays, which have resulted in a rich magnetic phase diagram and controversial explanations in the literature. Our systematic investigation of pure and impure Ru-1222 samples shows that the phase purity plays a vital role in understanding the true magnetic behavior of the system. In the past, experimental studies have been carried out on the Ru-1222 sample with different purity levels. Therefore, different interpretations have been given to explain the magnetic properties of the Ru-1222 material. Our investigation shows that Ru-1222 consists of Ru-1212 as a prominent impurity phase, which significantly alters the magnetic and transport properties of this material. Both 1222 and 1212 have similar magnetic behavior, with only the magnetic transition temperatures being different. The superposition of magnetic signals from Ru-1222 and Ru-1212 leads to a small peak at about 124 K in the ZFC curve similar to that of an impure sample. The reopening of hysteresis loops above 90 K and the double superconducting transition observed in impure Ru-1222 are also due to the interference between 1222 and 1212 phases. The Ru-1212 impurity phase could be decomposed by increasing the final sintering temperature to more than 1080 °C. The phase pure Ru-1222 sample obtained has a single magnetic transition close to 90 K, a significantly suppressed coercivity at $90 \text{ K} \leq T \leq 200 \text{ K}$, and a single superconducting transition.

In spite of the successful explanation of the magnetic behavior in Ru systems, however, a different magnetic behavior may be hypothesized as follows. If we take into account the possible magnetic properties of the 1222/1212 systems from the point of view of their similarities with high- T_c superconductors (basically, we imply the properties of a CuO_2 plane),^{29,30} then we may end up with the need to explicitly specify the charge carrier concentration in the system. Indeed, depending on the concentration, our system may have superconducting, ferromagnetic, and antiferromagnetic properties within the CuO_2 plane.²⁹⁻³² In this case, our consideration, which refers to the magnetic behavior governed by the RuO planes, may need to be superposed with the magnetic behavior ruled by the CuO_2 planes. However, this kind of study is beyond the scope of the present paper.

ACKNOWLEDGMENTS

The authors would like to thank J. Park for assistance with SEM observations. This work is financially supported by the Australian Research Council.

- ¹For a review, see Topics in Current Physics Vols. 32 and 34, edited by Ø. Fischer and M. B. Maple (Springer-Verlag, New York, 1983).
- ²J. W. Lynn, S. Skanthakumar, Q. Huang, S. K. Sinha, Z. Hossain, L. C. Gupta, R. Nagarajan, and C. Godart, Phys. Rev. B **55**, 6584 (1997).
- ³I. Felner, U. Asaf, Y. Levi, and O. Millo, Phys. Rev. B **55**, R3374 (1997).
- ⁴J. Kikas, A. Laisaar, A. Suisalu, A. Kuznetsov, and A. Ellervee, Phys. Rev. B **57**, 14 (1998).
- ⁵C. Bernhard, J. L. Tallon, Ch. Niedermayer, Th. Blasius, A. Golnik, E. Brücher, R. K. Kremer, D. R. Noakes, C. E. Stronach, and E. J. Ansaldo, Phys. Rev. B **59**, 14099 (1999).
- ⁶A. C. McLaughlin, W. Zhou, J. P. Attfield, A. N. Fitch, and J. L. Tallon, Phys. Rev. B **60**, 7512 (1999).
- ⁷J. W. Lynn, B. Keimer, C. Ulrich, C. Bernhard, and J. L. Tallon, Phys. Rev. B **61**, R14964 (2000).
- ⁸Y. Tokunaga, H. Kotegawa, K. Ishida, Y. Kitaoka, H. Takagiwa, and J. Akimitsu, Phys. Rev. Lett. **86**, 5767 (2001).
- ⁹I. Felner, E. Galstyan, and I. Nowik, Phys. Rev. B **71**, 064510 (2005).
- ¹⁰I. Felner, E. Galstyan, R. H. Herber, and I. Nowik, Phys. Rev. B **70**, 094504 (2004).
- ¹¹C. A. Cardoso, F. M. Araujo-Moreira, V. P. S. Awana, E. Takayama-Muromachi, O. F. de Lima, H. Yamauchi, and M. Karppinen, Phys. Rev. B **67**, 020407(R) (2003).
- ¹²C. A. Cardoso, A. J. C. Lanfredi, A. J. Chiquito, F. M. Araujo-Moreira, V. P. S. Awana, H. Kishan, R. L. de Almeida, and O. F. de Lima, Phys. Rev. B **71**, 134509 (2005).
- ¹³Y. Y. Xue, D. H. Cao, B. Lorenz, and C. W. Chu, Phys. Rev. B **65**, 020511(R) (2001).
- ¹⁴Y. Y. Xue, B. Lorenz, D. H. Cao, and C. W. Chu, Phys. Rev. B **67**, 184507 (2003).
- ¹⁵G. V. M. Williams and S. Krämer, Phys. Rev. B **62**, 4132 (2000).
- ¹⁶N. Balchev, B. Kunev, J. Pirov, G. Mihova, and K. Nenkov, Mater. Lett. **59**, 2357 (2005).
- ¹⁷A. Shengelaya, R. Khasanov, D. G. Eschenko, I. Felner, U. Asaf, I. M. Savic, H. Keller, and K. A. Müller, Phys. Rev. B **69**, 024517 (2004).
- ¹⁸R. Nigam, A. V. Pan, and S. X. Dou, J. Appl. Phys. **101**, 09G109 (2007).
- ¹⁹I. Felner, E. B. Sonin, T. Machi, and N. Koshizuka, Physica C **341-348**, 715 (2000).
- ²⁰P. Kameli, H. Salamati, and M. Eslami, Solid State Commun. **137**, 30 (2006).
- ²¹G. Cao, S. McCall, and J. E. Crow, Phys. Rev. B **55**, R672 (1997).
- ²²I. Felner, U. Asaf, S. Reich, and Y. Tsabba, Physica C **311**, 163 (1999).
- ²³L. Klein, J. S. Dodge, C. H. Ahn, G. J. Snyder, T. H. Geballe, M. R. Beasley, and A. Kapitulnik, Phys. Rev. Lett. **77**, 2774 (1996).
- ²⁴A. V. Pan, S. Zhou, H. Liu, and S. Dou, Supercond. Sci. Technol. **16**, L33 (2003).
- ²⁵A. V. Pan and S. X. Dou, J. Appl. Phys. **96**, 1146 (2004).
- ²⁶M. Matvejeff, V. P. S. Awana, L.-Y. Jang, R. S. Liu, H. Yamauchi, and M. Karppinen, Physica C **392-396**, 87 (2003).
- ²⁷E. Kneller, A. Seeger, and H. Kronmüller, *Ferromagnetismus* (Springer, Berlin, 1962).
- ²⁸J. Crangle, *Solid State Magnetism* (Arnold, London, 1991).
- ²⁹H. J. Kang, P. Dai, J. W. Lynn, M. Matsuura, J. R. Thompson, S. C. Zhang, D. N. Argyriou, Y. Onose, and Y. Tokura, Nature (London) **423**, 522 (2003).
- ³⁰K. Yamada, C. H. Lee, K. Kurahashi, J. Wada, S. Wakimoto, S. Ueki, H. Kimura, Y. Endoh, S. Hosoya, G. Shirane, R. J. Birgeneau, M. Greven, M. A. Kastner, and Y. J. Kim, Phys. Rev. B **57**, 6165 (1998).
- ³¹M. A. Kastner, R. J. Birgeneau, G. Shirane, and Y. Endoh, Rev. Mod. Phys. **70**, 897 (1998).
- ³²S. Katano, M. Sato, K. Yamada, T. Suzuki, and T. Fukase, Phys. Rev. B **62**, R14677 (2000).